J|A|C|S
ARTICLES
Published on Web 01/13/2006

Double-Ink Dip-Pen Nanolithography Studies Elucidate Molecular Transport

Jennifer R. Hampton,† Arrelaine A. Dameron, and Paul S. Weiss*

Contribution from the Departments of Chemistry and Physics, The Pennsylvania State University, University Park, Pennsylvania 16802−6300

Received September 15, 2005; E-mail: stm@psu.edu

Abstract: We have investigated the transport mechanism of the inks most typically used in dip-pen nanolithography by patterning both 16-mercaptohexadecanoic acid (MHDA) and 1-octadecanethiol (ODT) on the same Au{111} substrate. Several pattern geometries were used to probe ink transport from the tip to the sample during patterning of both dots (stationary tip) and lines (moving tip). When ODT was written on top of a pre-existing MHDA structure, the ODT was observed at the outsides of the MHDA structure, and the transport rate increased. In the reverse case, the MHDA was also observed on the outsides of the previously patterned ODT features; however, the transport rate was reduced. Furthermore, the shapes of pre-existing patterns of one ink were not changed by deposition of the other ink. These results highlight the important role hydrophobicity plays, both of the substrate as well as of the inks, in determining transport properties and thereby patterns produced in dip-pen nanolithography.

Introduction

The direct writing of material from the tip of an atomic force microscope (AFM) to a substrate was first shown in 1995 by Jaschke and Butt.[1] This observation was then developed by Mirkin and co-workers into a robust patterning technique, which has come to be known as dip-pen nanolithography (DPN).[2,3] The first DPN experiments used alkanethiols as "inks" on a gold substrate;[3] however the technique has since been extended to a variety of ink−substrate combinations, including polymers, biological molecules, and colloidal particles on semiconductors, oxides, and noble metals.[2] To date, the applications of DPN range from lithographic resists[4−6] to biologically compatible surfaces.[7−9]

The most studied DPN systems are thiol-containing molecules, in particular 16-mercaptohexadecanoic acid (MHDA) and 1-octadecanethiol (ODT), on Au surfaces. These two inks have been the subject of many investigations, in particular examining the influence of environmental conditions, such as relative humidity and temperature, on the writing process.[10−14] Most recently, the structures produced when patterning with a tip that had been coated with two inks have also been explored.[15] However, there have been comparatively few studies of the effect of the *surface* on both DPN ink transport from the tip to the surface and ink diffusion across the surface.

Here, we present the results of DPN experiments where both MHDA and ODT were written on the same area of a Au substrate. By patterning the surface with one ink and *subsequently* writing on top of that structure with a second ink (rather than patterning with two inks simultaneously[15]), we have examined the role surface hydrophobicity plays in determining ink transport in DPN. In addition, we have established that during DPN, inks flow across a pre-existing surface monolayer and adsorb at the edge of the pattern rather than diffuse through the existing self-assembled monolayer (SAM).

2. Experimental Methods

All DPN experiments were performed using a ThermoMicroscopes Autoprobe CP Research AFM (Veeco Instruments, Santa Barbara, CA) in contact mode. The AFM was enclosed in a glovebag (Spilfyter, VWR, West Chester, PA) for environmental control. Before each experiment and during tip or sample exchange, the glovebag was purged with dry inert gas to maintain constant atmospheric conditions. All experiments were performed at a relative humidity of 21 ± 1% and temperature of 24 ± 1 °C.

† Present address: Department of Physics, Washington and Jefferson College, Washington, PA 15301.
‡ Department of Chemistry.

(1) Jaschke, M.; Butt, H. J. *Langmuir* **1995**, *11*, 1061.
(2) Ginger, D. S.; Zhang, H.; Mirkin, C. A. *Angew. Chem., Int. Ed.* **2004**, *43*, 30.
(3) Piner, R. D.; Zhu, J.; Xu, F.; Hong, S. H.; Mirkin, C. A. *Science* **1999**, *283*, 661.
(4) Weinberger, D. A.; Hong, S. G.; Mirkin, C. A.; Wessels, B. W.; Higgins, T. B. *Adv. Mater.* **2000**, *12*, 1600.
(5) Zhang, H.; Chung, S. W.; Mirkin, C. A. *Nano Lett.* **2003**, *3*, 43.
(6) Zhang, H.; Lee, K. B.; Li, Z.; Mirkin, C. A. *Nanotechnology* **2003**, *14*, 1113.
(7) Cheung, C. L.; Camarero, J. A.; Woods, B. W.; Lin, T. W.; Johnson, J. E.; De Yoreo, J. J. *J. Am. Chem. Soc.* **2003**, *125*, 6848.
(8) Lee, K. B.; Park, S. J.; Mirkin, C. A.; Smith, J. C.; Mrksich, M. *Science* **2002**, *295*, 1702.
(9) Smith, J. C.; Lee, K. B.; Wang, Q.; Finn, M. G.; Johnson, J. E.; Mrksich, M.; Mirkin, C. A. *Nano Lett.* **2003**, *3*, 883.
(10) Peterson, E. J.; Weeks, B. L.; De Yoreo, J. J.; Schwartz, P. V. *J. Phys. Chem. B* **2004**, *108*, 15206.
(11) Rozhok, S.; Piner, R.; Mirkin, C. A. *J. Phys. Chem. B* **2003**, *107*, 751.
(12) Schwartz, P. V. *Langmuir* **2002**, *18*, 4041.
(13) Sheehan, P. E.; Whitman, L. J. *Phys. Rev. Lett.* **2002**, *88*, 156104.
(14) Weeks, B. L.; Noy, A.; Miller, A. E.; De Yoreo, J. J. *Phys. Rev. Lett.* **2002**, *88*, 255505.
(15) Salaita, K.; Amarnath, A.; Maspoch, D.; Higgins, T. B.; Mirkin, C. A. *J. Am. Chem. Soc.* **2005**, *127*, 11283.

10.1021/ja056369b CCC: $33.50

Commercially available Au{111} on mica substrates (Molecular Imaging, Tempe, AZ) were cleaned with UV/ozone just prior to use.[16] The MHDA and ODT molecules were purchased from Sigma-Aldrich (St. Louis, MO) and used as received. Silicon−nitride-coated plank-style cantilevers with a force constant of 0.05 N/m (Mikromasch, Portland, OR) were used both to write the desired patterns (using molecularly coated, hereafter referred to as "inked," cantilevers) and to image the resulting structures (using un-inked cantilevers). All cantilevers were cleaned with UV/ozone just prior to inking. Inking was performed in base-bath-cleaned (KOH/saturated ethanol) glass vials.

Cantilevers were inked with ODT by vapor deposition in sealed vials. The cantilever was exposed to sublimed ODT at 78 °C for ∼10 min and then left in the sealed container at room temperature until the ODT recrystallized (∼5 min). Cantilevers inked with MHDA were prepared following the "double dipping" procedure from a 5 mM acetonitrile solution of MHDA.[17] The cantilevers were dipped in the MHDA solution for ∼5 s, dried with inert gas, exposed to 18 MΩ water vapor for 5 min, allowed to air-dry for an additional 5 min, re-dipped in the MHDA solution for ∼5 s, and dried with inert gas.

Dip-pen nanolithography writing was performed using the Nanolithography module in the ProScan software package (Veeco Instruments, Santa Barbara, CA). Each pattern consisted of groups of "dots" (the shape defined by static-tip ink deposition) and/or "lines" (the shape defined by moving-tip ink deposition). For double-ink experiments, an alignment mark was written along with the first structure (a few tens of μm away) for nanoscale alignment of subsequent cantilevers.

Imaging of the DPN-generated structures was performed with un-inked cantilevers in a lateral force microscopy (LFM) mode. In the LFM images presented in this paper, a brighter display represents areas of higher frictional force between the tip and the sample, whereas a darker display represents lower friction. Areas patterned with MHDA appear with higher friction (and are thus displayed as brighter) than the surrounding gold because of the protruding carboxylic acid groups, whereas ODT areas image with lower friction (and are displayed as darker) than the surrounding gold.

Using Matlab (MathWorks, Natick, MA), the pattern areas were determined from the LFM images by one of two methods. In one method, a binary image was generated from the LFM image and a user-defined threshold. Each distinct feature in the binary image was then labeled separately. The number of pixels in each labeled feature was then counted, and the area of each was determined on the basis of the size of the image. The other method was used for the dot features only. In this case, three points were defined along the perimeter of the dot. From these points, a circle defining the dot was generated. The number of pixels that fell within the defined circle was counted, and the area was determined in the same manner as the first method. For circular features, both methods gave the same area within a few pixels.

Figure 1 illustrates the stages of a double-ink experiment where ODT dots were patterned on top of MHDA dots. At each stage in the experiment, the patterned features were imaged in LFM mode with a clean, un-inked cantilever, and these images are shown in the figure. Figure 1A shows five MHDA dots (patterned with identical dwell times of 356 s, chosen to pattern nominally 2-μm diameter dots) after the MHDA patterning step. Dots M1 and M3 are the dots on which ODT was subsequently written, and dots M2 and M4 are dots that were used for reference after the ODT patterning. Dot M5 is an additional alignment dot closer to the experimental pattern, used for final alignment verification. Figure 1B shows the full structure after the ODT was patterned. Here, ODT was patterned on top of dots M1 and M3 (dots O*1 and O*3, respectively) using two different dwell times (236 and 943 s, chosen to pattern nominally 2- and 4-μm diameter dots, respectively). The same dwell times were used to pattern additional reference dots of ODT (dots O*2 and O*4, respectively). Henceforth,

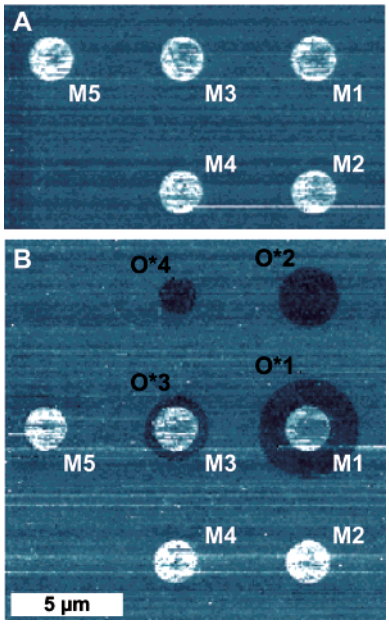

Figure 1. Extracts from two 20 μm × 20 μm lateral force microscopy images showing the stages of a double-ink dip-pen nanolithography experiment. (A) Five dots of MHDA (M1−M5) patterned with identical dwell times of 356 s. (B) Four dots of ODT (O*1−O*4), two of which (O*1 and O*3) were patterned on top of the previously patterned MHDA dots (M1 and M3). Dots O*1 and O*2 were patterned with the same dwell time of 943 s, and dots O*3 and O*4 were patterned with the same dwell time of 236 s. Imaging conditions: scan rate 4 Hz, force setpoint 1 nN.

all DPN-generated objects are labeled in a similar manner. "M" ("O") indicates that the structure was patterned with MHDA (ODT); no asterisk (asterisk) indicates that the structure was patterned in the first (second) step.

This same general procedure was used for all the double-ink experiments discussed below. Single-ink control experiments were also performed using the same method, but without switching inks between the two patterning steps.

3. Results

3.1. Double-Ink Stationary Tip Experiments. Figure 2 shows the results of two double-ink dot-on-top-of-dot experiments of the type shown in Figure 1, where ODT was patterned on top of MHDA (A) and MHDA was patterned on top of ODT (B). Dots M1 and M2 (O1 and O2) were patterned in the first step with identical dwell times (356 s for MHDA and 236 s for ODT, chosen to pattern nominally 2-μm diameter dots in both cases), and then dots O*1 and O*2 (M*1 and M*2) were patterned in the second step, again with identical dwell times (943 s for ODT and 1146 s for MHDA, chosen to pattern nominally 4-μm diameter dots in both cases). In both cases, the result of the second patterning step (O*1 or M*1) was a region of the second ink on the outside of the previously patterned feature (M1 or O1, respectively). From this observation, we conclude that for DPN of MHDA and ODT, both inks diffuse from the AFM tip on top of the pre-existing self-assembled monolayer and adsorb to the bare surface at the periphery of the feature.

For each experiment, the areas of the patterned regions of MHDA and ODT were calculated. Because the ink transport rate in DPN varies from experiment to experiment, the areas of the patterned regions are not useful by themselves. Instead, we define a relative transport rate, $R_{I^*|I}$, which compares the

(16) Ron, H.; Rubinstein, I. *Langmuir* **1994**, *10*, 4556.
(17) NanoInk, personal communication.

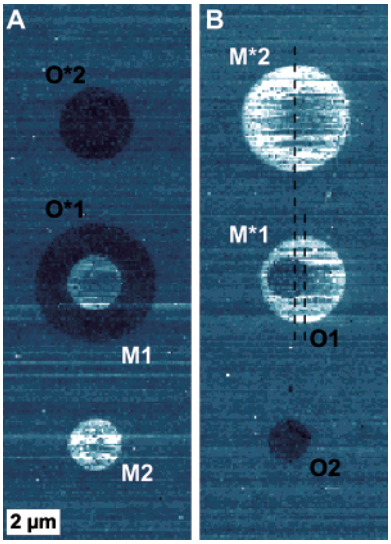

Figure 2. Extracts from two 20 μm × 20 μm lateral force microscopy images from double-ink dip-pen nanolithography experiments. (A) First, the middle (M1) and lower (M2) MHDA dots were patterned with identical dwell times of 356 s. Then, the middle (O*1), on top of M1, and upper (O*2) ODT dots were patterned with identical dwell times of 943 s. (B) First, the middle (O1) and lower (O2) ODT dots were patterned with identical dwell times of 236 s. Then, the middle (M*1), on top of O1, and upper (M*2) MHDA dots were patterned with identical dwell times of 1146 s. The two vertical dotted lines show the horizontal locations of the center of the M*2 dot (longer line) and the M*1 dot (shorter line). Note that the small shift in registration of the patterning locations (longer line) was amplified in the results of that patterning (shorter line). Imaging conditions: scan rate 4 Hz, force setpoint 1 nN.

transport for the ink *I** (O* for ODT or M* for MHDA) on a surface patterned with the ink *I* (M or O, respectively) to the transport of *I** on the bare Au surface during the same experiment. For each ink combination,

$$R_{I^*|I} = \frac{A_{I^*|I}}{A_{I^*|\mathrm{Au}}} \qquad (1)$$

where $A_{I^*|I}$ is the area of *I** that was patterned on top of *I* and $A_{I^*|\mathrm{Au}}$ is the area of the reference dot of *I** patterned on bare Au using the same dwell time in the same experiment. If ink transport were not affected by the presence of the patterned feature already on the surface, the relative transport rate calculated in this way would be unity.

For ODT writing on MHDA, $R_{\mathrm{O}^*|\mathrm{M}} = 1.8 \pm 0.6$. In contrast, for MHDA writing on ODT, $R_{\mathrm{M}^*|\mathrm{O}} = 0.39 \pm 0.14$. This large difference in relative transport rates is strong evidence that the nature of the substrate plays a crucial role during ink transport in DPN. In particular, ODT transport is sped up when writing on MHDA compared to that when writing on bare Au, whereas MHDA transport is slowed when writing on ODT.

This observation helps explain why the O1/M*1 structure in Figure 2B is not symmetric. The two dotted lines in Figure 2B show the horizontal locations of the center of the M*2 dot (longer line) and the M*1 dot (shorter line). The longer dotted line does not pass through the center of the O1 dot, indicating there was a small shift to the right in the registration between patterning ODT in the first step and patterning MHDA in the second step. However, the shorter line is even farther to the right of the center of the O1 dot, showing that the small shift in registration of the patterning locations was amplified in the results of that patterning. Because transport of MHDA was inhibited when patterning on ODT, small differences in the symmetry of the pattern were amplified.

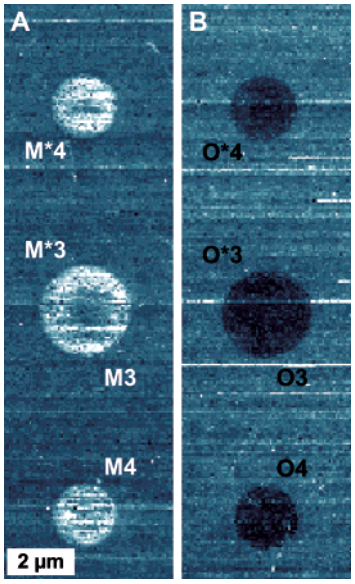

Figure 3. Extracts from two 17 μm × 17 μm lateral force microscopy images from two single-ink dip-pen nanolithography experiments. Four dots of MHDA (A) and ODT (B) were patterned in two steps. First, the middle (M3 or O3) and lower (M4 or O4, respectively) dots were patterned with identical dwell times (404 s for MHDA and 217 s for ODT). Then, the middle (M*3 or O*3, respectively), on top of M3 or O3, respectively, and upper (M*4 or O*4, respectively) dots were patterned with identical dwell times (404 s for MHDA and 217 s for ODT). Imaging conditions: scan rate 4 Hz, force setpoint 1 nN.

3.2. Single-Ink Stationary Tip Control Experiments. As a control experiment for the double-ink dot-on-top-of-dot experiments, analogous single-ink experiments were performed using the method shown in Figure 1 but without changing the ink between the two patterning steps. Figure 3 shows the results of this two-step patterning with MHDA (A) and ODT (B). Dots M3 and M4 (O3 and O4) were patterned in the first step with identical dwell times (404 s for MHDA and 217 s for ODT, chosen to pattern nominally 2-μm diameter dots in both cases), and then dots M*3 and M*4 (O*3 and O*4) were patterned in the second step, again with identical dwell times (404 s for MHDA and 217 s for ODT, chosen to pattern nominally 2-μm diameter dots in both cases).

For each single-ink experiment, the areas of the individual patterned features were calculated. In each case, the area of the reference dot from the first patterning step (dot 4 in Figure 3) was subtracted from the area of the dot patterned in two steps (dot 3/*3). The result represents the additional ink patterned in the second step on top of the already-patterned ink, $A_{I^*|I}$. This area was compared to the area, $A_{I^*|\mathrm{Au}}$, of the reference dot from the second patterning step (dot *4). For each single-ink experiment, the relative transport rate was calculated from these areas using Equation 1. If transport were not affected by the ink already on the surface, then the sum of the areas of dot 4 and dot *4 would be equal to the area of dot 3/*3, and $R_{I^*|I}$ would be equal to 1.

For MHDA writing on already-patterned MHDA, $R_{\mathrm{M}^*|\mathrm{M}} = 1.02 \pm 0.04$, indicating that MHDA transport is not affected by MHDA already on the surface, within the error of the measurement. In contrast, $R_{\mathrm{O}^*|\mathrm{O}} = 0.82 \pm 0.08$, indicating that ODT transport is slowed slightly by the presence of the already-patterned ODT.

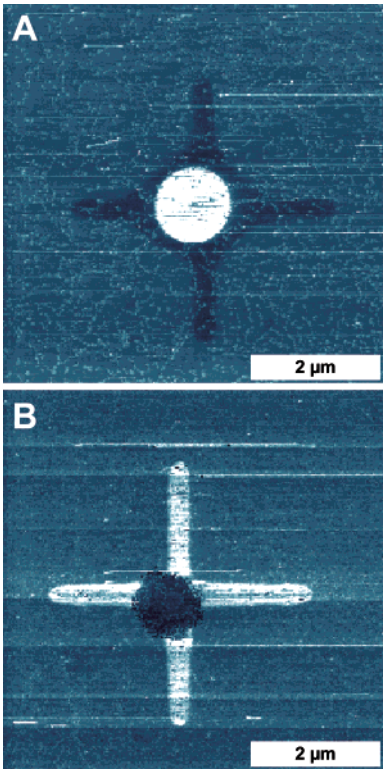

Figure 4. Two 6 μm × 6 μm lateral force microscopy images from double-ink dip-pen nanolithography experiments. (A) Cross of ODT patterned on an MHDA dot. (B) Cross of MHDA patterned on an ODT dot. Imaging conditions: scan rate 4 Hz, force setpoint 1 nN.

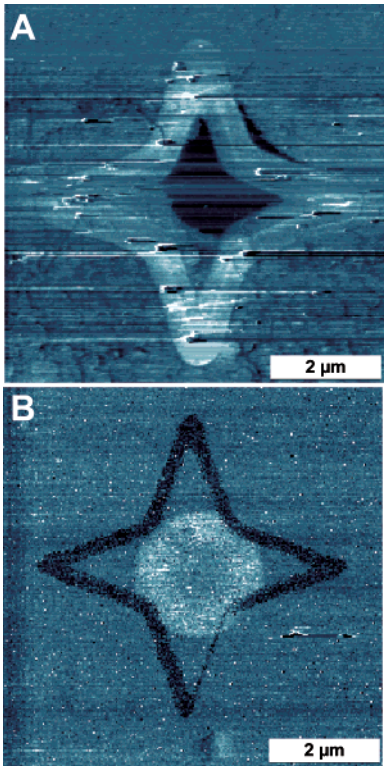

Figure 5. Two 7 μm × 7 μm lateral force microscopy images from double-ink dip-pen nanolithography experiments. (A) Dot of ODT patterned in an MHDA corral. (B) Dot of MHDA patterned in an ODT corral. Imaging conditions: scan rate 4 Hz, force setpoint 1 nN.

3.3. Double-Ink Moving Tip Experiments. Figure 4 shows results from double-ink experiments where an ODT cross was patterned on top of an MHDA dot (A) and an MHDA cross was patterned onto an ODT dot (B). This geometry is similar to the dot-on-top-of-dot geometry, except that in the second patterning step, the tip was moved across the patterned feature rather than being stationary. In the case of ODT patterning on top of MHDA (Figure 4A), the ODT was deposited in a ring around the outside of the MHDA dot in addition to the cross structure. In the opposite case (Figure 4B), the MHDA was deposited only as the specified cross feature.

This difference is consistent with the results seen in the double-ink dot-on-top-of-dot experiments, where the relative transport rate for ODT patterning on MHDA, $R_{O^*,M}$, was larger than 1, whereas the reverse relative transport rate, $R_{M^*,O}$, was smaller than 1. When the ODT-inked tip encountered the already-patterned MHDA feature, the transport rate increased and the ink diffused in all directions across the top of the existing MHDA, resulting in ODT around the periphery of the dot. In the opposite case, the MHDA transport decreased when patterning on the ODT dot, resulting in no MHDA at the outside of the ODT dot except in the directions of the cross structure.

3.4. Double-Ink Corrals. Figure 5 shows results from double-ink experiments where an ODT dot was patterned inside an MHDA star-shaped corral (A) and an MHDA dot was patterned inside an ODT star-shaped corral (B). In this geometry, the second ink was not patterned on top of the first ink, as in the previous geometries. Instead, the geometry was designed to determine how the ink behaves when it encounters an already-deposited area of the other ink when moving laterally on the substrate. In both cases, the dot was patterned on a bare Au surface, but it was large enough that the ink encountered the corral during the course of the deposition.

In Figure 5A, the ODT did not deposit in a radially symmetric fashion. Instead, the transport was inhibited in the directions in which the MHDA corral was encountered and deposited preferentially in the directions of bare Au substrate (where the corral was farther away). The interaction of the ODT with the MHDA corral did not change the shape of the corral. However, a small amount of ODT also reached the outside of the corral. Similar conclusions can be drawn from Figure 5B. The MHDA deposited preferentially in the directions with the longest distance to the ODT corral. In addition, a small amount of MHDA reached the exterior of the ODT corral perimeter. The ODT corral shape was not altered as a result of the MHDA deposition. In both cases shown in Figure 5, there was no indication that the inks mixed within the lines of the corrals.

4. Discussion

The double-ink experiments shown here give a comprehensive picture of ink transport for the most common inks used in DPN. In particular, these results establish that during DPN, ink molecules travel from the molecularly coated tip to the surface and across any preexisting SAM where they deposit at the periphery of the structure. In this respect, the results for all the geometries investigated are consistent. When one ink is deposited on top of the other, as in Figures 2 and 4, the new ink deposits on the edge of the preexisting structure. When one ink encounters an obstacle of the other, as in Figure 5, the ink eventually deposits on the other side of the obstacle. In both cases, there is no evidence of mixing between the two inks or of one ink pushing the other ink out of the way.

By measuring the relative transport rates from the dot-on-top-of-dot experiments, we have shown that ODT transport is increased when patterning on MHDA and that MHDA transport is inhibited when patterning on ODT. The asymmetries in transport evident in the other double-ink experiments can be explained by the differences in transport rates when patterning on a surface with an existing SAM and when patterning on a bare surface.

The advancing contact angle for water on a bare Au surface is 30−70°,[18] whereas on single-component ODT and MHDA SAMs formed on Au, the contact angles are 115 and <15°, respectively.[19] Thus, in a DPN experiment, a region patterned with MHDA is more hydrophilic than the surrounding Au, whereas a region patterned with ODT is more hydrophobic. These differences in hydrophobicity between the three surfaces affect the size and shape of the water meniscus that can form between an AFM tip and the surface during DPN.[20] On a surface patterned with MHDA, the water meniscus spreads out, whereas on a surface with ODT, the water meniscus is compact, if it exists at all.

The solubility of MHDA in water is over 100 times larger than that of ODT, due to the carboxylic acid terminal group.[21,22] Thus, the ink molecules on an AFM cantilever interact with the water meniscus differently in these two systems. In particular, when patterning with MHDA, the ink molecules prefer to be in the water meniscus, especially in the case of a hydrophobic surface. When patterning with ODT, however, the ink molecules will be less likely to be in the meniscus and prefer to be either on the tip or the surface, forming micelles to minimize water exposure (decreasing the energy of the system) in the interim.

The concentration of the molecules in the meniscus is unknown. However, considering that the ODT crystals are visible on the microscale whereas the water meniscus is not, the ODT concentration is assumed to be higher than the critical micelle concentration. Additionally, the MHDA concentration may also be above the critical micelle concentration, in which case these molecules would also form micelles in the meniscus.[23−25]

We propose a mechanism based on the above for the differences in transport rates of these two molecules when patterning on the other. When ODT is patterned on top of MHDA, the water meniscus spreads out, and the insoluble ink molecules are transported more easily, resulting in a higher transport rate. When MHDA is patterned on top of ODT, the water meniscus is compact, and transport of the more soluble ink molecules is inhibited, resulting in a lower transport rate. This proposed mechanism is shown schematically in Figure 6.

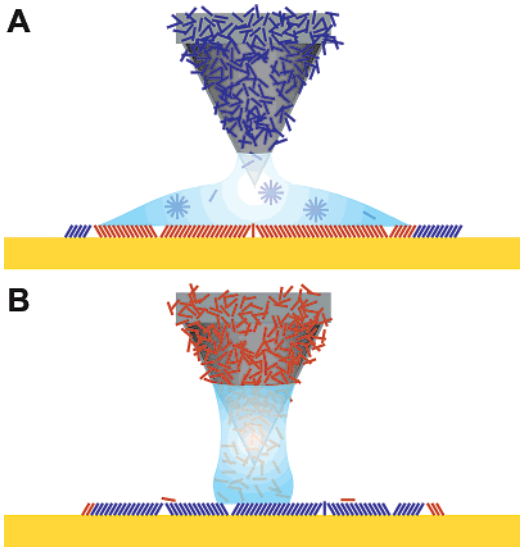

Figure 6. Schematics depicting the proposed mechanism for the subsequent deposition in double-ink DPN. (A) ODT patterned on top of MHDA. The water meniscus spreads out on the MHDA surface, facilitating ODT transport. (B) MHDA patterned on top of ODT. The water meniscus beads up on the on ODT surface, hindering MHDA transport.

This mechanism is consistent with the recent results by Mirkin and co-workers where both ODT and MHDA were deposited simultaneously from a double-inked DPN tip.[15] In that case, MHDA, which interacts strongly with the water meniscus, deposits more quickly than ODT, resulting in MHDA at the center of the structure. The deposition of ODT then occurs at the periphery.

5. Conclusions

Through a series of double-ink dip-pen nanolithography experiments, we have shown that ink transport in DPN is highly dependent on the exact nature of the patterning surface. The *rate* and *direction* of transport as well as the ability of the ink to pattern at all are affected by adsorbates on the surface (whether patterned intentionally or present due to insufficient cleaning or ambient contamination). These facts can explain both the variability in experimental results for DPN to date, even for nominally identical inking protocols and environmental conditions, and the lack of mixing between ODT and MHDA observed in the present experiments.

In our proposed mechanism for the changes in the ink transport rate, both the water solubility of the ink molecules and the hydrophobicity of the surface affect the resulting transport. Thus, the interactions of the water meniscus with both the ink molecules and the substrate play important roles in determining the ink transport.

Dip-pen nanolithography has been touted as an ideal patterning tool for high-density structures, particularly for biological materials.[2] The results shown here indicate that the presence of one ink affects the patterning of additional inks, especially for molecules with different functional groups in close proximity. In order for DPN to be technologically viable, a fundamental understanding of the roles of the interactions between the materials patterned with DPN will be required.

(18) Bain, C. D.; Troughton, E. B.; Tao, Y. T.; Evall, J.; Whitesides, G. M.; Nuzzo, R. G. *J. Am. Chem.* Soc. **1989**, *111*, 321.
(19) Laibinis, P. E.; Whitesides, G. M. *J. Am. Chem. Soc.* **1992**, *114*, 1990.
(20) The role of the water meniscus in ink transport during DPN, particularly when patterning at low relative humidity, is controversial. However, at the relative humidity of our experiments (21%), there is no dispute that a meniscus forms.
(21) *Handbook of Physical Properties of Organic Chemicals*; Howard, P. H., Meylan, W. M., Eds.; CRC Press: Boca Raton, FL, 1997.
(22) Meylan, W. M.; Howard, P. H.; Boethling, R. S. *Environ. Toxicol. Chem.* **1996**, *15*, 100.
(23) Southall, N. T.; Dill, K. A.; Haymet, A. D. J. *J. Phys. Chem. B* **2002**, *106*, 521.
(24) Tanford, C. *J. Phys. Chem.* **1974**, *78*, 2469.
(25) Tanford, C. *The Hydrophobic Effect: Formation of Micelles and Biological Membranes*, 2nd ed.; John Wiley and Sons: New York, 1980.

Acknowledgment. We thank Xiaomei Li and Valeriy Gorbunov from Veeco Instruments for the use of the beta version of their nanolithography software. The Air Force Office of Scientific Research, Army Research Office, Defense Advanced Research Projects Agency, National Science Foundation, Office of Naval Research, and Semiconductor Research Corporation are gratefully acknowledged for their support.

JA056369B